



Published in final edited form as:

Pflugers Arch. 2009 April ; 457(6): 1253–1263. doi:10.1007/s00424-008-0600-8.

Slow Inactivation of the NaV1.4 Sodium Channel in Mammalian Cells Is Impeded by Co-Expression of the β 1 Subunit

Jadon Webb¹, Fen-fen Wu², and Stephen C. Cannon^{1,2}

¹Neuroscience Program, UT Southwestern Medical Center, Dallas, Texas 75390

²Department of Neurology, UT Southwestern Medical Center, Dallas, Texas 75390

Abstract

In response to sustained depolarization or prolonged bursts of activity in spiking cells, sodium channels enter long-lived non-conducting states from which recovery at hyperpolarized potentials occurs over hundreds of milliseconds to seconds. The molecular basis for this slow inactivation remains unknown, although many functional domains of the channel have been implicated. Expression studies in *Xenopus* oocytes and mammalian cell lines have suggested a role for the accessory β 1 subunit in slow inactivation, but the effects have been variable. We examined the effects of the β 1 subunit on slow inactivation of skeletal muscle (Nav1.4) sodium channels expressed in HEK cells. Co-expression of the β 1 subunit impeded slow inactivation elicited by a 30 sec depolarization, such that the voltage dependence was right shifted (depolarized) and recovery was hastened. Mutational studies showed this effect was dependent upon the extracellular Ig-like domain, but was independent of the intracellular C-terminal tail. Furthermore, the β 1 effect on slow inactivation was shown to be independent of the negative coupling between fast and slow inactivation.

Keywords

gating; SCN; SCN1B; mammalian expression system; skeletal muscle; voltage-gated sodium channel

Introduction

Slow inactivation is a universal feature of voltage-gated Na channels wherein after a sustained depolarization recovery from inactivation occurs over hundreds of msec to seconds [32]. Slow inactivation is functionally important for setting the fractional availability of channels in response to sustained shifts in the resting potential or for regulating cellular excitability in response to prolonged bursts of action potentials [30]. Moreover, defects in slow inactivation contribute to the pathogenesis human disorders affecting skeletal muscle, heart, and brain [3]. These observations have stimulated many investigations to gain some understanding of the molecular mechanism underlying this slow gating process, but as of yet

Corresponding Author: Stephen C. Cannon, M.D., Ph.D., Professor and Chairman, Department of Neurology, University of Texas Southwestern Medical Center, 5323 Harry Hines Blvd, Dallas, TX 75390-8813, Phone: (214) 645-6225, Fax: (214) 645-6236, Steve.Cannon@UTSouthwestern.edu.

no structural details or conceptual models have emerged that provide a firm understanding of the conformational changes that cause slow inactivation. The challenge has been that perturbations at many different domains of the channel affect slow inactivation, including the outer vestibule of the pore [1], selectivity filter [40, 41], inner vestibule, S6 segments [39, 43], and voltage sensor domains [14, 22]. Another complexity is that several distinct kinetic components of slow inactivation may be revealed, depending of the specific voltage protocol.

The objective of this study was to clarify further the role of the accessory $\beta 1$ subunit on slow inactivation of the skeletal muscle Na channel, NaV1.4, expressed in a mammalian cell line, and thereby add to the growing knowledgebase that will shape the development of a mechanistic understanding. The $\beta 1$ subunit is expressed in brain, peripheral nerve, skeletal muscle, and heart where it forms a non-covalent association with the pore-forming α subunit [11]. The $\beta 1$ subunit is a single-pass transmembrane protein with an extracellular amino terminus that forms an Ig-like domain important for interacting with cell adhesion molecules and extracellular matrix, and a short intracellular carboxyl tail [10]. The α subunit alone is capable of forming functional voltage-gated Na channels. Co-expression of the $\beta 1$ subunit increases cell surface expression levels and modulates channel gating. The effects of $\beta 1$ are most prominent in the *Xenopus* oocyte expression system, where channels comprised of the α subunit alone have a markedly decreased rate of whole-cell current decay during a test depolarization (~ 5 -fold slower than for native channels in mammalian cells), and co-expression of α and $\beta 1$ subunits results in heteromeric channels that inactivate with fast kinetics comparable to that observed in mammalian cells [5, 11]. The oocyte system has been used to examine the effects of $\beta 1$ subunit co-expression on slow inactivation, but the results have been conflicting with some reports of enhancement [41] whereas others have reported disruption of slow inactivation [1, 35]. In mammalian cell lines, Na currents inactivate rapidly even if only the α subunit alone is expressed [37]. Co-expression of the $\beta 1$ subunit has a negligible effect on the rate of onset for fast inactivation for neuronal, cardiac, or skeletal muscle Na channels [20, 38, 45]. Varied effects have been observed for other aspects of fast inactivation in mammalian cells, with co-expression of $\beta 1$ producing either enhanced fast inactivation (left shift of voltage dependence and slower recovery for NaV1.2 or NaV1.3 in CHO cells [21]) or impediment of fast inactivation (right shift of voltage-dependence and faster recovery for cardiac > skeletal [38] or neuronal NaV1.2 [45] channels). Even less is known about the effects of $\beta 1$ coexpression on slow inactivation in mammalian systems, with a single study showing impeded slow inactivation (right-shifted voltage dependence, faster recovery) for neuronal NaV1.2 channels [45]. The only other study to examine the effects of $\beta 1$ co-expression on Na channel (NaV1.4 and NaV1.5) slow inactivation in a mammalian system did not use a hyperpolarizing gap pulse to remove fast inactivation [38], and therefore it was not possible to separate the effects of fast from slow inactivation in the voltage-dependence protocol.

We have examined the effect of $\beta 1$ subunit on slow inactivation of human skeletal muscle sodium channels (Nav1.4) transiently expressed in a mammalian cell line (HEK293). In agreement with prior work on Nav1.2 [45], co-expression of the $\beta 1$ subunit mildly impeded slow inactivation, as revealed by enhanced recovery and a depolarized shift in voltage dependence. Furthermore, we found that the N-terminal C121W mutation disrupted this

effect, whereas deletion of the entire C-terminus left $\beta 1$ function intact. Additional studies with mutated Nav1.4 α subunits also show that this effect is independent of the negative coupling between fast and slow inactivation.

Materials and Methods

Construction of plasmids

The cDNA for the human sodium channel α -subunit (Nav1.4) was kindly provided by A.L. George in plasmid pRc/CMV-hSkM1 [4]. The human sodium channel $\beta 1$ subunit cDNA [18] was subcloned into the EcoR1 site of the mammalian expression plasmid pcDNA3.1(+) (Invitrogen, Carlsbad, CA). The C-terminal deletion of the $\beta 1$ subunit ($\beta 1$ /CTdel, deletion of amino acids 185–218) was generated as described previously [5]. Site-directed mutagenesis was performed according to the manufacturer's protocol (QuikChange™ Stratagene, La Jolla, CA) to generate the N-terminal cysteine to tryptophan missense mutation in the $\beta 1$ subunit ($\beta 1$ /C121W) and the domain III-IV loop mutation F1311C in Nav1.4 (α /F1311C). The mutated constructs were sequenced in both directions to confirm the presence of the mutation and to ensure that no other mutations were introduced during the site-directed mutagenesis.

Expression of sodium channels

Human embryonic kidney cells (HEK293) were transiently transfected with various combinations of α and $\beta 1$ subunits, using the calcium phosphate method [8]. Briefly, α -subunit containing plasmid (either wild-type or mutant α /F1311C) at a concentration of 0.2 μ g per 35-mm dish was co-transfected with four-fold molar excess $\beta 1$ -subunit plasmid (wild-type or mutant), as well as a CD8 marker (0.2 μ g per 35-mm dish). After 24–72 hours, cells were trypsinized and passaged to 12-mm round glass cover slips for electrophysiological recording. Individual transfection-positive cells were identified by labeling with anti-CD8 antibody cross-linked to microbeads [13] (Invitrogen, Carlsbad, CA).

Whole-cell recording

Na^+ currents were measured with standard whole-cell recording techniques as previously described [8]. Recordings were made with an Axopatch 200A amplifier controlled by pClamp 9.0 (Molecular Devices, Sunnyvale, CA). The output was filtered at 5 kHz and digitally sampled at 50 kHz using a DigiData 1200 Series interface (Molecular Devices). More than 70% of the series resistance was compensated by the analog circuitry of the amplifier and leakage conductance was corrected by digital scaling and subtraction of passive current elicited by hyperpolarizing voltage steps applied from the holding potential. To minimize the effects of small endogenous currents and avoid residual effects from series resistance, only cells with peak currents between 0.5 nA and 15 nA at -10 mV were included. After initially establishing whole-cell access, we often observed an increase in the size of the peak current, as well as a leftward shift in the voltage dependence of activation and fast inactivation. To standardize responses across cells, we waited at least 10 min after gaining whole-cell access before recording.

Patch electrodes were fabricated from borosilicate capillary tubes with a multi-stage puller (Sutter, Novato, CA). The shank of the pipette was coated with Sylgard and the tip was heat-polished to a final tip resistance (in bath solution) of 0.5–1.5 M Ω . The pipette (internal) solution contained (mM): CsF 105, NaCl 35, EGTA 5, and Cs-HEPES 10 (pH 7.4). Fluoride was used in the pipette to prolong seal stability. The bath solution contained (mM): NaCl 140, KCl 4, CaCl₂ 2, MgCl₂ 1, glucose 2.5, and Na-HEPES 10 (pH 7.4). [2-(Trimethylammonium) ethyl]methanethiosulfonate Bromide (MTS-ET) (Toronto Research Chemicals, North York, Ontario, Canada) was kept dry in small aliquots and diluted to 500 μ M in internal pipette solution immediately before use. Recordings were made at room temperature (24–28°C).

Data analysis

Analysis of raw current traces was performed manually off-line using Clampfit 9.0 (Molecular Devices). Reduced data were then analyzed and plotted in Origin 6.1 (Microcal, Northampton, MA). The voltage-dependence of steady-state slow inactivation was fitted to a Boltzmann function plus a non-zero pedestal (I_0) calculated as $I/I_{PEAK} = (1 - I_0)/[1 + \exp((V - V_{1/2})/k)] + I_0$, where $V_{1/2}$ is the half-maximum voltage and k is the slope factor. The time constant of entry to fast inactivation was measured as the monoexponential decay of currents elicited at –10 mV, as measured between 90% and 10% of the peak current. Data from a series of peak currents undergoing entry to slow inactivation were fit with a monoexponential decay to determine the time constant. Recovery from slow inactivation showed two components, and was fit with a biexponential function. Symbols with error bars indicate means \pm S.E.M. Statistical significance was determined by the Student's unpaired t -test with p -values noted in the text.

Results

While the primary objective of this study was to test for the influence of the $\beta 1$ subunit on slow inactivation of sodium channels expressed in mammalian cells, we also characterized fast gating behavior to explicitly define how accessory subunit expression or mutations in the α or $\beta 1$ subunit affected activation and fast inactivation in the HEK cell expression system, which may secondarily influence slow inactivation gating [7, 29].

Activation and fast inactivation

Robust sodium currents with comparable maximal peak current amplitudes were observed in HEK cells transfected with the α subunit only (Nav1.4), $\alpha + \beta 1$, or $\alpha +$ either of the two mutant $\beta 1$ subunit constructs (Figure 1A). The peak Na current density at a test potential of –15 mV for cells transfected with $\beta 1$ subunit constructs was not different from cells transfected with Nav1.4 alone (Table. 1). The voltage dependence of activation was not appreciably affected by coexpression of wild-type or mutant $\beta 1$ subunits, as shown by the superposition of the peak current – voltage data in Figure 1 B.

The kinetics of entry to fast inactivation from the open state was determined by fitting the current decay elicited by step depolarizations from –120 mV to between –40 and +75 mV with a monoexponential time course. Time constants (τ_h) were similar for the Nav1.4 α -

subunit expressed alone or coexpressed with WT or mutant $\beta 1$ subunits (Figure 1C). Recovery from fast inactivation was determined by a two-pulse protocol. A 30-ms conditioning pulse to 0 mV was applied to fully fast inactivate channels, followed by a recovery gap to -120 mV for a variable duration, and finally a test pulse to -10 mV to assay availability as the peak Na current. Recovery of the peak Na current as a function of gap duration was fit with a monoexponential function. Recovery time constants at -120 mV were indistinguishable between HEK cells transfected with α -subunit alone or cotransfected with WT $\beta 1$, $\beta 1/CTdel$, or $\beta 1/C121W$ (Table 1).

The voltage-dependence of steady-state fast inactivation was measured as the relative peak current elicited after 300 ms conditioning pulses to voltages ranging from -120 to -50 mV. Data were fit with a Boltzmann function for each cell individually and the sets of parameter values for each channel type were compared to cells transfected with only the α subunit (Figure 2 and Table 1). Coexpression of WT $\beta 1$ or the C-terminal deletion construct ($\beta 1/CTdel$) both caused a small $+5$ mV ($p < 0.01$) depolarized shift in the half-inactivation voltage ($V_{1/2}$). Co-transfection of the $\beta 1$ N-terminal mutant ($\beta 1/C121W$) yielded $V_{1/2}$ results intermediate to α -subunit alone and $\alpha + \beta 1$. In addition, the slope factor (k) was reduced compared to $\alpha + \beta 1$ WT ($p < 0.05$).

These data show that channels containing WT $\beta 1$ and the C-terminal deletion construct $\beta 1/CTdel$ have similar fast inactivation gating behavior, as has been reported in the oocyte expression system where the effects are more prominent [5]; whereas mutation of the extracellular N-terminus disrupts $\beta 1$ function and results in gating properties more similar to currents observed when the α -subunit alone is expressed [5, 19, 42]. Because transfection of all three $\beta 1$ subunit constructs (WT, $\beta 1/CTdel$, $\beta 1/C121W$) produced a detectable change of fast inactivation, we conclude each of these constructs was expressed and formed heteromeric complexes with the α -subunit at the plasma membrane. Some caution is in order with regard to the $\beta 1/C121W$ mutant construct, however, as other studies in oocytes have demonstrated that these mutant subunits are ineffective at forming functional heterodimeric channels (possibly due to impairment of either trafficking or dimeric association) [21]. Indeed, the intermediate behavior for the fast inactivation data in Fig. 2 can be fit reasonably well by a combination of two channel types: 60% with $V_{1/2}$ comparable $\alpha\beta 1$ dimers and 40% monomeric channels (dashed line in Fig. 2). Nevertheless, these observations on fast-gating behavior imply we can test for modulatory effects on slow inactivation for all three $\beta 1$ subunit constructs. Finally, these data also show that the effect of exogenously transfected $\beta 1$ expression is detectable, despite the possible small contribution from a low level expression of endogenous $\beta 1a$ splice variants in HEK cells [24].

Steady-state slow inactivation

The voltage-dependence of steady-state slow inactivation was measured using a series of 30 s conditioning pulses to voltages ranging from -120 to 0 mV. Each conditioning pulse was followed by a 20-ms gap at -120 mV to allow full recovery from fast inactivation (time constant ~ 2 ms, Table 1) before a test depolarization was applied to measure slow inactivation as the reduction in peak current (Fig. 3 A, *inset*). Peak currents elicited by the test pulse were normalized to the maximum available current elicited from a holding

potential of -120 mV. The voltage-dependence measured for a series of conditioning depolarizations was then fit with a Boltzmann function with a non-zero pedestal. Voltage of half-inactivation ($V_{1/2}$) for steady-state slow inactivation was depolarized (right-shifted, Fig. 3) by $+10.5$ mV upon coexpression of WT $\beta 1$ ($p < 0.005$). Co-transfection of the $\beta 1$ C-terminal deletion ($\beta 1/\text{CTdel}$) yielded results similar to WT $\beta 1$, whereas co-transfection of the N-terminal $\beta 1$ mutant ($\beta 1/\text{C121W}$) produced channels with a voltage dependence similar to that when NaV1.4 alone was expressed. The slope factor (k) was not significantly affected by any condition tested: α : $V_{1/2} = -61.4 \pm 2.1$ mV, $k = 12.3 \pm 1.0$ mV, $n = 5$; $\alpha + \beta 1$: $V_{1/2} = -50.9 \pm 0.8$ mV, $k = 11.7 \pm 0.39$ mV, $n = 5$; $\alpha + \beta 1/\text{C121W}$: $V_{1/2} = -59.0 \pm 1.3$ mV, $k = 12.1 \pm 0.82$, $n = 5$; $\alpha + \beta 1/\text{CTdel}$: $V_{1/2} = -52.9 \pm 1.7$ mV, $k = 11.7 \pm 0.51$ mV, $n = 5$. The maximal extent of slow inactivation, I_o as measured at a conditioning voltage of 0 mV, was not statistically different among the various $\beta 1$ subunit constructs: α : 0.076 ± 0.013 ; $\alpha + \beta 1/\text{C121W}$: 0.098 ± 0.0097 ; $\alpha + \beta 1$: 0.064 ± 0.0051 ; $\alpha + \beta 1/\text{CTdel}$: 0.11 ± 0.014 .

Entry to slow inactivation

The rate of entry to slow inactivation was measured with a sequential-pulse protocol (Figure 4, *inset*). The holding potential was stepped to 0 mV to inactivate Na^+ channels. Next, a series of paired-pulses was applied to measure the extent of slow inactivation at varying times after this shift in holding potential. The paired-pulses consisted of a brief recovery gap to -120 mV for 20 ms to allow complete recovery from fast inactivation and a brief 3 ms test depolarization to -10 mV to measure the available Na current (fraction not slow-inactivated). Peak current during the test pulse was normalized to the maximal current observed when the conditioning pulse was omitted and averaged data are shown in Figure 4 for each of the $\beta 1$ constructs. Solid lines show monoexponential fits to the data. The rate of entry to slow inactivation was not affected by coexpression of WT $\beta 1$ or the $\beta 1$ C-terminal deletion ($\beta 1/\text{CTdel}$) in comparison to the data for the α -subunit alone. The $\beta 1$ N-terminal mutant ($\beta 1/\text{C121W}$), however, prolonged the entry rate by 1.4-fold ($p < 0.05$). Estimated values for the entry time constants were: α : 1780 ± 193 ms, $n = 5$; $\alpha + \beta 1$: 1640 ± 121 ms, $n = 6$; $\alpha + \beta 1/\text{C121W}$: 2470 ± 208 ms, $n = 5$; $\alpha + \beta 1/\text{CTdel}$: 1740 ± 132 ms, $n = 5$.

Recovery from slow inactivation

The time course for recovery of sodium channel availability upon repolarization after prolonged depolarization is the critical defining feature that distinguishes among the multiple components of inactivation described for sodium channels. We measured recovery following conditioning pulses to 0 mV of either 3 s or 30 s duration. This strategy was designed to optimize the sensitivity of examining the two most prominent components: recovery from intermediate inactivation, I_M , with a time course on the order of 200 msec; recovery from slow inactivation, I_S , with a time course on the order of 3 s. It was not practical to study ultraslow inactivation in our preparation because even with conditioning pulses of 60 s only a very small fraction ($< 5\%$) of the current recovered with the kinetics of ultraslow inactivation (> 10 sec).

Recovery from slow inactivation at -120 mV was measured with a sequential recovery protocol, in which a series of brief test pulses (3 ms, -10 mV) were applied at progressively longer times after a long conditioning pulse to 0 mV (either 3 s or 30 s). Control

experiments verified that the brief repeated excursions to -10 mV did not alter the time course of recovery in comparison to the more laborious technique of measuring a single point along the recovery trajectory and then reapplying the conditioning pulse to reset the level of inactivation before the next test pulse. After a 3 s conditioning pulse (Fig. 5 A), about 75% of channels were slow inactivated, consistent with the entry data shown in Figure 4. Recovery at -120 mV after the initial 20 ms had a dominant exponential component with a time constant of ~ 200 ms, indicating that channels were in the intermediate state of slow inactivation (I_M). The recovery data were tightly clustered and there was no statistical difference in recovery time constant from WT (Table 2). Following a 30 s conditioning pulse (Fig. 5 B), the recovery after the initial 20 ms had two clearly distinguishable components. The faster component recovered with a time constant of ~ 200 ms which we interpret as recovery from I_M , and the slower component recovered with a time constant on the order of 15 s which we interpret as channels recovering from the I_S state. The maximal extent of slow inactivation (I_M plus I_S) at the end of the 30 s conditioning pulse was comparable for all $\beta 1$ constructs tested, as shown by the overlap of data for the initial recovery point at 20 ms in Figure 5B. Similarly, the time constants were not affected by co-expression of the $\beta 1$ subunit (Table 2). The large difference in recovery behavior was attributable to partitioning of channels among I_M and I_S states. Co-expression of WT $\beta 1$ or the C-terminal deletion mutation $\beta 1/CTdel$ impeded entry to I_S within the 30 s conditioning pulse. Figure 5C shows the fraction of channels partitioned into I_S , as determined from the bi-exponential fits, was about 0.3 for these constructs, whereas in the absence of $\beta 1$ co-expression or for the $\beta 1/C121W$ mutation the fraction in I_S was 0.43 (Table 2).

Removal of fast inactivation does not abolish the $\beta 1$ effect on slow inactivation

The possibility that the $\beta 1$ effect on slow inactivation may occur through coupling of fast and slow inactivation was tested with a mutant α -subunit construct that abolished fast-inactivation. The rationale is based on prior observations of negative coupling between fast and slow inactivation. The initial observation was made in squid giant axon internally perfused with pronase, which abolished fast inactivation but slow inactivation persisted and the onset was two-fold faster [29]. Disruption of fast inactivation by mutating the IFM \rightarrow QQQ motif in the III-IV linker increases the maximal extent of slow inactivation and accelerates the rate of onset for Nav1.4 or Nav1.5 expressed in oocytes [7, 28]. Conversely, the $\beta 1$ subunit enhances fast inactivation for many expression systems, especially frog oocytes [5, 11], although this effect was not apparent for the HEK cell studies herein. Nevertheless, the fact that coupling between fast and slow inactivation is firmly established raises the question of whether the $\beta 1$ impediment of slow inactivation observed herein is dependent upon intact fast inactivation. To test this possibility, we disrupted the sodium channel III-IV loop fast inactivation gate and measured the effects of coexpression of WT $\beta 1$ on steady-state slow inactivation. Nav1.4 channels with the IFM \rightarrow QQQ mutation express poorly in HEK cells, and therefore we used an F1311C mutant that expresses reasonably well and has a complete loss of fast inactivation upon intracellular exposure to the thiol cross-linking reagent MTS-ET.

Peak Na current amplitudes were reduced ~ 10 -fold in HEK cells transfected with Nav1.4/F1311C compared to WT. Addition of 5 μ M MTS-ET to the pipette solution produced a

dramatic loss of fast inactivation, as shown in Figure 6A. The voltage-dependence of steady-state slow inactivation in MTS-ET modified F1311C channels, with and without co-expression of WT $\beta 1$, was measured with a 15 s conditioning pulse as described for above. Co-expression of the WT $\beta 1$ subunit impeded slow inactivation, even in the absence of fast inactivation, as shown by the +8 mV rightward shift ($p < 0.005$) of the data for F1311C + WT $\beta 1$ channels in Figure 6B. The $V_{1/2}$ and k values for the Boltzmann fits were: F1311C: $V_{1/2} = -59.3 \pm 1.3$ mV, $k = 6.98 \pm 1.54$ mV, $n = 4$; F1311C + $\beta 1$: $V_{1/2} = -51.0 \pm 1.1$ mV, $k = 4.89 \pm 0.34$, $n = 4$.

Discussion

A widely-accepted conceptual model of the mechanism by which voltage-gated sodium channels undergo slow inactivation has not yet emerged, despite much effort and the use of a variety of experimental approaches. Several lines of evidence implicate the pore, in the region of the selectivity filter [1, 35, 41] or adjacent areas in S6 segments [25, 39], as the critical region that undergoes a conformational change resulting in a non-conducting slow-inactivated state(s). These observations have led to speculation that slow inactivation of sodium channels shares mechanistic features in common with C-type inactivation of Kv channels, for which several lines of evidence are consistent with a model wherein constriction at the outer vestibule of the pore prevents conduction [6, 16], although the inner cavity between the selectivity filter and activation gate also undergoes structural changes [26]. There are some glaring differences for C-type inactivation in Kv channels, however, compared to the properties of slow inactivation for NaV channels, which suggest the molecular mechanisms may share little in common between the two channel types. First, unlike C-type inactivation for Kv channels [16], there is little evidence for an external foot-in-the door effect that impedes slow inactivation for WT NaV channels (but see [36]). Second, sites in the external vestibule within one residue of the DEKA selectivity filter are accessible to modification by MTS-ET in the (intermediate) slow-inactivated state [34]. Third, manipulations from the internal side of the NaV selectivity filter may have large effects on slow inactivation; such as batrachotoxin binding [44] which is the only modification known to completely remove slow inactivation, mutations in S6 segments [25, 39], or lidocaine acting as an internal foot-in-the door to impede ultra-slow inactivation of K1237E mutant Nav1.4 channels [31].

Given the uncertainty surrounding the mechanism of slow inactivation for NaV channels, we designed the present study to address the more focused question of whether the accessory $\beta 1$ subunit has a role in slow inactivation of Nav1.4 channels, and if so what domain of $\beta 1$ is critical for this effect? Several prior studies have characterized the effects of the accessory $\beta 1$ subunit expression on activation and fast inactivation, [5, 11, 12, 27], and to a lesser extent on slow inactivation [1, 35, 41, 45]. Most of the studies on $\beta 1$ and slow inactivation were performed in the oocyte expression system, where the effects of $\beta 1$ co-expression on fast gating are very prominent. A serious limitation of the studies in oocytes, is that they have an anomalous slow mode of fast inactivation gating [5, 23] that has kinetic features similar to the “intermediate” component of slow inactivation, I_M [2, 9], but bears an uncertain relation to true slow inactivation. I_M is defined operationally as the component that recovers with a time constant of 100–300 msec at -120 mV, whereas the slow component I_S

recovers over 1 – 3 s and ultraslow, I_S recovers at times > 10 s. The anomalous slow mode and I_M are clearly different, as can be distinguished for example with trains of brief test depolarizations which cause a modal shift in gating (from slow to fast) for α -subunit only channels expressed in oocytes, but not $\alpha/\beta 1$ heteromeric channels [5]. In our view, while studies of slow inactivation on $\alpha/\beta 1$ heteromeric NaV channels can be performed in the oocyte expression system, the observations on slow gating for α -subunit homomeric channels are difficult, if not impossible, to interpret. Therefore, we used a mammalian expression system (transient transfection in HEK cells) to characterize the effects of $\beta 1$ subunit co-expression on slow inactivation.

A primary finding of this study is that co-expression of the $\beta 1$ accessory subunit mildly impedes slow inactivation of skeletal muscle Nav1.4 channels expressed in a mammalian cell background, similar to prior work in the neuronal Nav1.2 [45], but see [21]. The disruption of slow inactivation by the $\beta 1$ subunit is manifest by a +10 mV rightward shift in steady-state voltage dependence (Figure 3) and a reduced propensity to partition into the slow-inactivated (I_S) state during a 30 s conditioning pulse (Figure 5B). Notice that a less comprehensive test of slow inactivation recovery would have missed the difference produced by co-expression of the $\beta 1$ subunit, as shown by the similarity of the responses following a 3 s conditioning pulse which primarily reflects occupancy of the intermediate inactivated, I_m state (Figure 5A). Aside from the caveats listed above for the interpretation of NaV slow-mode gating in oocytes, our results in HEK cells are in agreement with two previous oocyte studies using Nav1.4 [1, 35] and a mammalian cell study using Nav1.2 [45] showing that co-expression of $\beta 1$ impedes slow inactivation; whereas an enhancement of slow inactivation by $\beta 1$ was reported for Nav1.4 (but no change for Nav1.5) in oocytes [41] or for Nav1.2 and Nav1.3 in CHO cells [21].

Mutational analysis has provided additional insights on the domain of the $\beta 1$ subunit that was required to modulate slow inactivation. Prior studies on $\beta 1$ function, based on assays of fast inactivation in the oocyte system, have shown that the cytoplasmic carboxyl tail (residues 185–218) is not required [5], whereas the large extracellular amino terminus has a critical Ig-like fold that when disrupted by mutation causes a total loss of the $\beta 1$ enhancement of fast inactivation [5, 19]. The present studies on modulation of slow inactivation in HEK cells are precisely concordant with the studies on modulation of fast inactivation: deletion of the entire cytoplasmic terminus does not alter modulation of slow inactivation ($\beta 1/CTdel$ impedes slow inactivation to the same extent as WT $\beta 1$), whereas the $\beta 1/C121W$ mutation that disrupts a critical disulfide bond in the extracellular Ig-like fold caused a loss of modulatory function. Importantly, for the same cells in which a failure to observe the modulatory right shift of slow inactivation by C121W occurred (Figure 3, inverted triangles), clear changes were present in the voltage dependence of fast inactivation (Figure 2). This concordance implies the lack of an effect by $\beta 1/C121W$ on slow inactivation was unlikely to be the result of a completely non-functional subunit. On the other hand, we acknowledge that the intermediate effects of mutant subunit expression observed for fast inactivation raise the possibility that $\beta 1/C121W$ expressed poorly or was less efficient in associating with the α subunit. Our findings are also in agreement with other work showing disruption of $\beta 1$ modulatory effects from another N-terminal (R85H) mutation [45]. Taken together, these observations on the importance of the extracellular

domain suggested that the effect of the β_1 subunit on slow inactivation may operate through coupling to fast inactivation. Namely, the mild impediment of slow inactivation from β_1 expression might be derived primarily from β_1 -enhancement of fast inactivation (which in turn is negatively coupled to slow inactivation). To explore this possibility, we introduced an α -subunit mutation to abolish fast inactivation and then examined the ability of β_1 expression to still modulate slow inactivation. Figure 6 shows that even in the absence of fast inactivation, co-expression of the β_1 subunit still disrupted slow inactivation. Some caution is warranted for this interpretation because the voltage-dependence with or without β_1 is right-shifted compared to WT Nav1.4 (compare to Figure 3), which raises the question of how the “slow” gating in channels with disrupted fast inactivation relates to normal slow inactivation for WT channels. Nevertheless, we interpret these data as supportive evidence for a model in which the β_1 subunit modulates slow inactivation by impeding occupancy of the I_S state, through α/β interactions in the transmembrane or extracellular domains, and that is independent of β_1 effects on fast inactivation. Studies of β_1 subunit effects on gating properties of Nav1.4 / Nav1.5 chimeras expressed in oocytes have suggested an interaction between the extracellular amino terminus of β_1 and the α subunit pore loops [17, 41], perhaps through the effect of negative charge on the A/A' strand of the Ig-like fold [19]. This observation fits well with the notion that conformational changes in the pore region are critical for slow inactivation [1, 35, 41], and therefore this interaction site may be the mechanism by which the β_1 subunit modulates slow inactivation gating.

The C121W mutation in the β_1 subunit is a cause of generalized epilepsy with febrile seizures plus, GEFS(+) [42]. Prior expression studies to explore the pathomechanism in this disorder have revealed a loss-of-function defect for fast inactivation, in that C121W fails to promote the fast mode of inactivation in oocytes [42], despite intact dimerization of the mutant β_1 subunit with neuronal α subunits [21]. While this effect is quite robust in the oocyte expression system, the relevance to NaV channel function in mammalian brain is less clear because the neuronal α subunit isoforms, as well as those for cardiac and skeletal muscle, all inactivate with rapid onset kinetics in mammalian expression systems without co-expression of β_1 [15, 33, 37]. Moreover, functional studies of β_1 - C121W co-expressed with neuronal Nav1.2 and Nav1.3 in CHO cells have revealed a different loss-of-function gating defect, wherein the enhancement of fast inactivation by WT β_1 (–10 mV left shift and slower recovery) does not occur with C121W, which would thereby theoretically increase neuronal excitability [21]. Our studies on gating modulation of Nav1.4 expressed in a mammalian cell line herein have identified another functional defect of C121W, failure to modulate slow inactivation. While this effect observed in the skeletal muscle α subunit isoform has yet to be confirmed for neuronal Na channels, this slow inactivation defect should also be considered to be a potential contributing factor to the pathogenesis of GEFS(+). Moreover, an additional β_1 mutation (R85C) associated with GEFS(+) fails to induce a rightward shift of slow inactivation for Nav1.2 channels [45]. In prior studies, we have shown by computer simulation that mild impairment of slow inactivation can have a profound effect on excitability [9]. Our data imply slow inactivation is predicted to be enhanced in neurons expressing the β_1 mutant C121W, which at first glance might be expected to reduce the susceptibility to epileptic discharges. This apparent paradox is reconciled by the observation that loss-of-function changes for neuronal Na channels, due to

mutations of the α subunit (Nav1.1 or Nav1.2), are clearly associated with an increased susceptibility to seizures [46].

Acknowledgements:

This work was supported by the NIAMS of the National Institutes of Health (AR42703 to SCC) and the Medical Scientist Training Program (T32 GM08014 to JW).

References

1. Balser JR, Nuss HB, Chiamvimonvat N, Perez-Garcia MT, Marban E and Tomaselli GF, External pore residue mediates slow inactivation in μ 1 rat skeletal muscle sodium channels. *J Physiol (Lond)*, 1996 494(Pt 2): p. 431–42. [PubMed: 8842002]
2. Benitah JP, Chen Z, Balser JR, Tomaselli GF and Marban E, Molecular dynamics of the sodium channel pore vary with gating: interactions between P-segment motions and inactivation. *J Neurosci*, 1999 19(5): p. 1577–85. [PubMed: 10024345]
3. Cannon SC, Slow inactivation of sodium channels: more than just a laboratory curiosity. *Biophys J*, 1996 71(1): p. 5–7.
4. Chahine M, Bennett PB, George AL, Jr. and Horn R, Functional expression and properties of the human skeletal muscle sodium channel. *Pflugers Archiv - European Journal of Physiology*, 1994 427(1–2): p. 136–42. [PubMed: 8058462]
5. Chen CF and Cannon SC, Modulation of Na^+ channel inactivation by the β 1 subunit: a deletion analysis. *Pflügers Archiv*, 1995 431: p. 186–195. [PubMed: 9026778]
6. Choi KL, Aldrich RW and Yellen G, Tetraethylammonium blockade distinguishes two inactivation mechanisms in voltage-activated K^+ channels. *Proc Natl Acad Sci U S A*, 1991 88(12): p. 5092–5. [PubMed: 2052588]
7. Featherstone DE, Richmond JE and Ruben PC, Interaction between fast and slow inactivation in SkM1 sodium channels. *Biophysical Journal*, 1996 71: p. 3098–3109. [PubMed: 8968581]
8. Hayward LJ, Brown RH, Jr. and Cannon SC, Inactivation defects caused by myotonia-associated mutations in the sodium channel III-IV linker. *J Gen Physiol*, 1996 107(5): p. 559–76. [PubMed: 8740371]
9. Hayward LJ, Brown RH, Jr. and Cannon SC, Slow inactivation differs among mutant Na channels associated with myotonia and periodic paralysis. *Biophysical Journal*, 1997 72: p. 1204–1219. [PubMed: 9138567]
10. Isom LL, Sodium channel beta subunits: anything but auxiliary. *Neuroscientist*, 2001 7(1): p. 42–54. [PubMed: 11486343]
11. Isom LL, De Jongh KS, Patton DE, Reber BF, Offord J, Charbonneau H, Walsh K, Goldin AL and Catterall WA, Primary structure and functional expression of the beta 1 subunit of the rat brain sodium channel. *Science*, 1992 256(5058): p. 839–42. [PubMed: 1375395]
12. Isom LL, Scheuer T, Brownstein AB, Ragsdale DS, Murphy BJ and Catterall WA, Functional co-expression of the beta 1 and type IIA alpha subunits of sodium channels in a mammalian cell line. *Journal of Biological Chemistry*, 1995 270(7): p. 3306–12. [PubMed: 7852416]
13. Jurman ME, Boland LM, Liu Y and Yellen G, Visual identification of individual transfected cells for electrophysiology using antibody-coated beads. *Biotechniques*, 1994 17(5): p. 876–81. [PubMed: 7840967]
14. Kontis KJ and Goldin AL, Sodium channel inactivation is altered by substitution of voltage sensor positive charges. *J Gen Physiol*, 1997 110(4): p. 403–13. [PubMed: 9379172]
15. Krafte DS, Volberg WA, Rapp L, Kallen RG, Lalik PH and Ciccarelli RB, Stable expression and functional characterization of a human cardiac Na^+ channel gene in mammalian cells. *J Mol Cell Cardiol*, 1995 27(2): p. 823–30. [PubMed: 7776389]
16. Liu Y, Jurman ME and Yellen G, Dynamic rearrangement of the outer mouth of a K^+ channel during gating. *Neuron*, 1996 16(4): p. 859–67. [PubMed: 8608004]

17. Makita N, Bennett PB and George AL, Jr., Molecular determinants of beta 1 subunit-induced gating modulation in voltage-dependent Na⁺ channels. *J Neurosci*, 1996 16(22): p. 7117–27. [PubMed: 8929421]
18. McClatchey AI, Cannon SC, Slaugenhaupt SA and Gusella JF, The cloning and expression of a sodium channel beta 1-subunit cDNA from human brain. *Human Molecular Genetics*, 1993 2(6): p. 745–9. [PubMed: 8394762]
19. McCormick KA, Isom LL, Ragsdale D, Smith D, Scheuer T and Catterall WA, Molecular determinants of Na⁺ channel function in the extracellular domain of the beta1 subunit. *J Biol Chem*, 1998 273(7): p. 3954–62. [PubMed: 9461582]
20. Meadows LS, Chen YH, Powell AJ, Clare JJ and Ragsdale DS, Functional modulation of human brain Nav1.3 sodium channels, expressed in mammalian cells, by auxiliary beta 1, beta 2 and beta 3 subunits. *Neuroscience*, 2002 114(3): p. 745–53. [PubMed: 12220575]
21. Meadows LS, Malhotra J, Loukas A, Thyagarajan V, Kazen-Gillespie KA, Koopman MC, Kriegler S, Isom LL and Ragsdale DS, Functional and biochemical analysis of a sodium channel beta1 subunit mutation responsible for generalized epilepsy with febrile seizures plus type 1. *J Neurosci*, 2002 22(24): p. 10699–709. [PubMed: 12486163]
22. Mitrovic N, George AL, Jr. and Horn R, Role of domain 4 in sodium channel slow inactivation. *J Gen Physiol*, 2000 115(6): p. 707–18. [PubMed: 10828245]
23. Moorman JR, Kirsch GE, VanDongen AMJ, Joho RH and Brown AM, Fast and slow gating of sodium channels encoded by a single mRNA. *Neuron*, 1990 4: p. 243–252. [PubMed: 2155011]
24. Moran O, Nizzari M and Conti F, Endogenous expression of the beta1A sodium channel subunit in HEK-293 cells. *FEBS Lett*, 2000 473(2): p. 132–4. [PubMed: 10812059]
25. O'Reilly JP, Wang SY and Wang GK, Residue-specific effects on slow inactivation at V787 in D2-S6 of Na(v)1.4 sodium channels. *Biophys J*, 2001 81(4): p. 2100–11. [PubMed: 11566781]
26. Panyi G and Deutsch C, Probing the cavity of the slow inactivated conformation of shaker potassium channels. *J Gen Physiol*, 2007 129(5): p. 403–18. [PubMed: 17438120]
27. Patton DE, Isom LL, Catterall WA and Goldin AL, The adult rat brain beta 1 subunit modifies activation and inactivation gating of multiple sodium channel alpha subunits. *Journal of Biological Chemistry*, 1994 269(26): p. 17649–55. [PubMed: 8021275]
28. Richmond JE, Featherstone DE, Hartman HA and Ruben PC, Slow Inactivation in Human Cardiac Sodium Channels. *Biophysical Journal*, 1998 74: p. 2945–2952. [PubMed: 9635748]
29. Rudy B, Slow Inactivation of the sodium conductance in squid giant axons. Pronase resistance. *Journal of Physiology*, 1978 283: p. 1–21. [PubMed: 722569]
30. Rudy B, Inactivation in Myxicola giant axons responsible for slow and accumulative adaptation phenomena. *J Physiol*, 1981 312: p. 531–49. [PubMed: 7265003]
31. Sandtner W, Szendroedi J, Zarrabi T, Zebedin E, Hilber K, Glaaser I, Fozzard HA, Dudley SC and Todt H, Lidocaine: a foot in the door of the inner vestibule prevents ultra-slow inactivation of a voltage-gated sodium channel. *Mol Pharmacol*, 2004 66(3): p. 648–57. [PubMed: 15322257]
32. Schauf CL, Pencek TL and Davis FA, Slow sodium inactivation in Myxicola axons. Evidence for a second inactive state. *Biophys J*, 1976 16(7): p. 771–8. [PubMed: 938717]
33. Scheuer T, Auld VJ, Boyd S, Offord J, Dunn R and Catterall WA, Functional properties of rat brain sodium channels expressed in a somatic cell line. *Science*, 1990 247(4944): p. 854–8. [PubMed: 2154850]
34. Struyk AF and Cannon SC, Slow inactivation does not block the aqueous accessibility to the outer pore of voltage-gated Na channels. *J Gen Physiol*, 2002 120(4): p. 509–16. [PubMed: 12356853]
35. Todt H, Dudley SC, Jr., Kyle JW, French RJ and Fozzard HA, Ultra-slow inactivation in mu1 Na⁺ channels is produced by a structural rearrangement of the outer vestibule. *Biophys J*, 1999 76(3): p. 1335–45. [PubMed: 10049317]
36. Townsend C and Horn R, Effect of alkali metal cations on slow inactivation of cardiac Na⁺ channels. *Journal of General Physiology*, 1997 110: p. 23–33. [PubMed: 9234168]
37. Ukomadu C, Zhou J, Sigworth FJ and Agnew WS, mu1 Na⁺ channels expressed transiently in human embryonic kidney cells: biochemical and biophysical properties. *Neuron*, 1992 8(4): p. 663–76. [PubMed: 1314619]

38. Valdivia CR, Nagatomo T and Makielski JC, Late Na currents affected by alpha subunit isoform and beta1 subunit co-expression in HEK293 cells. *J Mol Cell Cardiol*, 2002 34(8): p. 1029–39. [PubMed: 12234772]
39. Vedantham V and Cannon SC, Rapid and slow voltage-dependent conformational changes in segment IVS6 of voltage-gated Na(+) channels. *Biophys J*, 2000 78(6): p. 2943–58. [PubMed: 10827974]
40. Vilin YY, Fujimoto E and Ruben PC, A single residue differentiates between human cardiac and skeletal muscle Na+ channel slow inactivation. *Biophys J*, 2001 80(5): p. 2221–30. [PubMed: 11325725]
41. Vilin YY, Makita N, George AL, Jr. and Ruben PC, Structural determinants of slow inactivation in human cardiac and skeletal muscle sodium channels. *Biophys J*, 1999 77(3): p. 1384–93. [PubMed: 10465750]
42. Wallace RH, Wang DW, Singh R, Scheffer IE, George AL, Jr., Phillips HA, Saar K, Reis A, Johnson EW, Sutherland GR, Berkovic SF and Mulley JC, Febrile seizures and generalized epilepsy associated with a mutation in the Na+-channel beta1 subunit gene SCN1B. *Nat Genet*, 1998 19(4): p. 366–70. [PubMed: 9697698]
43. Wang SY and Wang GK, A mutation in segment I-S6 alters slow inactivation of sodium channels. *Biophys J*, 1997 72(4): p. 1633–40. [PubMed: 9083667]
44. Wang SY and Wang GK, Point mutations in segment I-S6 render voltage-gated Na+ channels resistant to batrachotoxin. *Proc Natl Acad Sci U S A*, 1998 95(5): p. 2653–8. [PubMed: 9482942]
45. Xu R, Thomas EA, Gazina EV, Richards KL, Quick M, Wallace RH, Harkin LA, Heron SE, Berkovic SF, Scheffer IE, Mulley JC and Petrou S, Generalized epilepsy with febrile seizures plus-associated sodium channel beta1 subunit mutations severely reduce beta subunit-mediated modulation of sodium channel function. *Neuroscience*, 2007 148(1): p. 164–74. [PubMed: 17629415]
46. Yu FH, Mantegazza M, Westenbroek RE, Robbins CA, Kalume F, Burton KA, Spain WJ, McKnight GS, Scheuer T and Catterall WA, Reduced sodium current in GABAergic interneurons in a mouse model of severe myoclonic epilepsy in infancy. *Nat Neurosci*, 2006 9(9): p. 1142–9. [PubMed: 16921370]

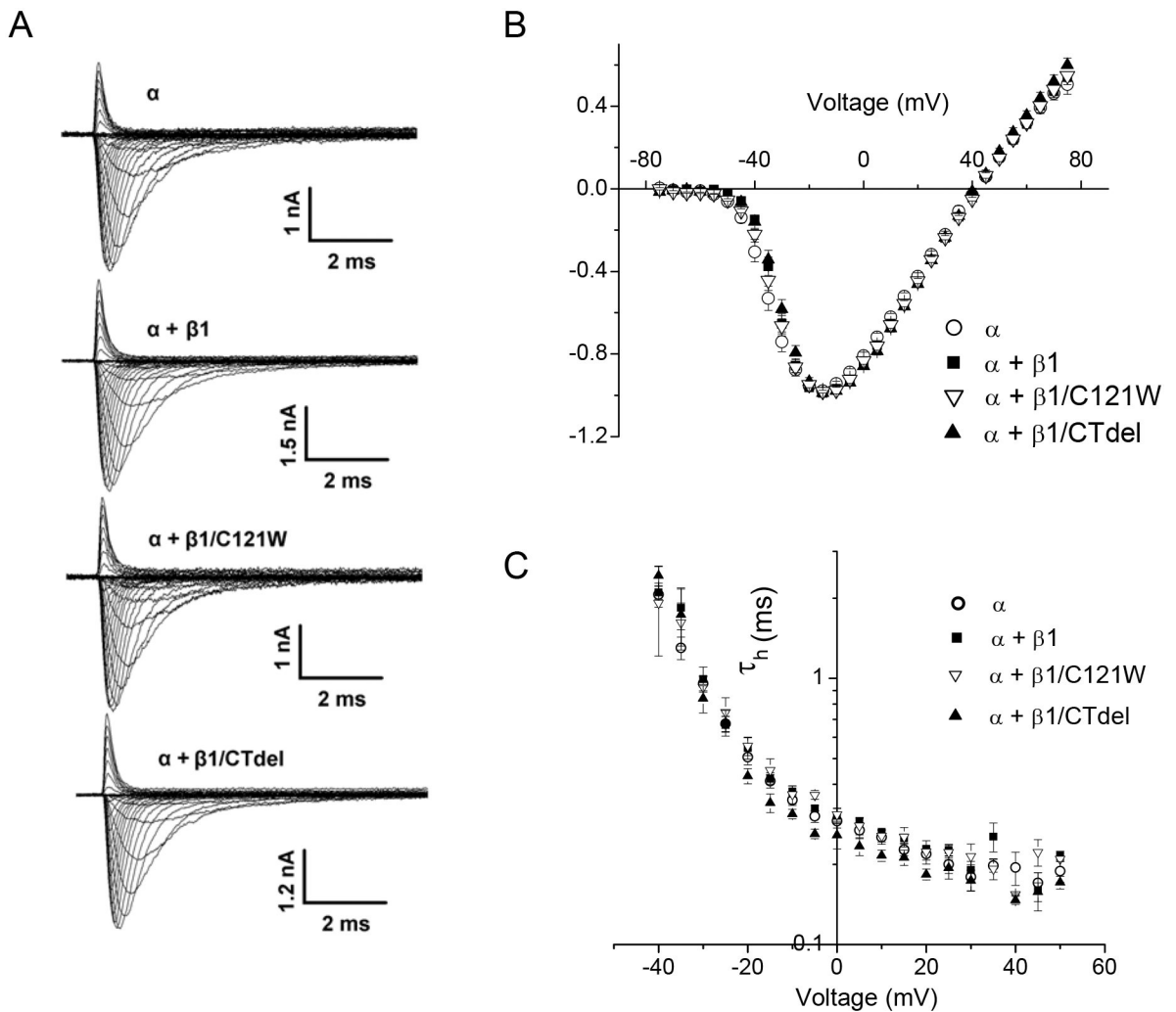
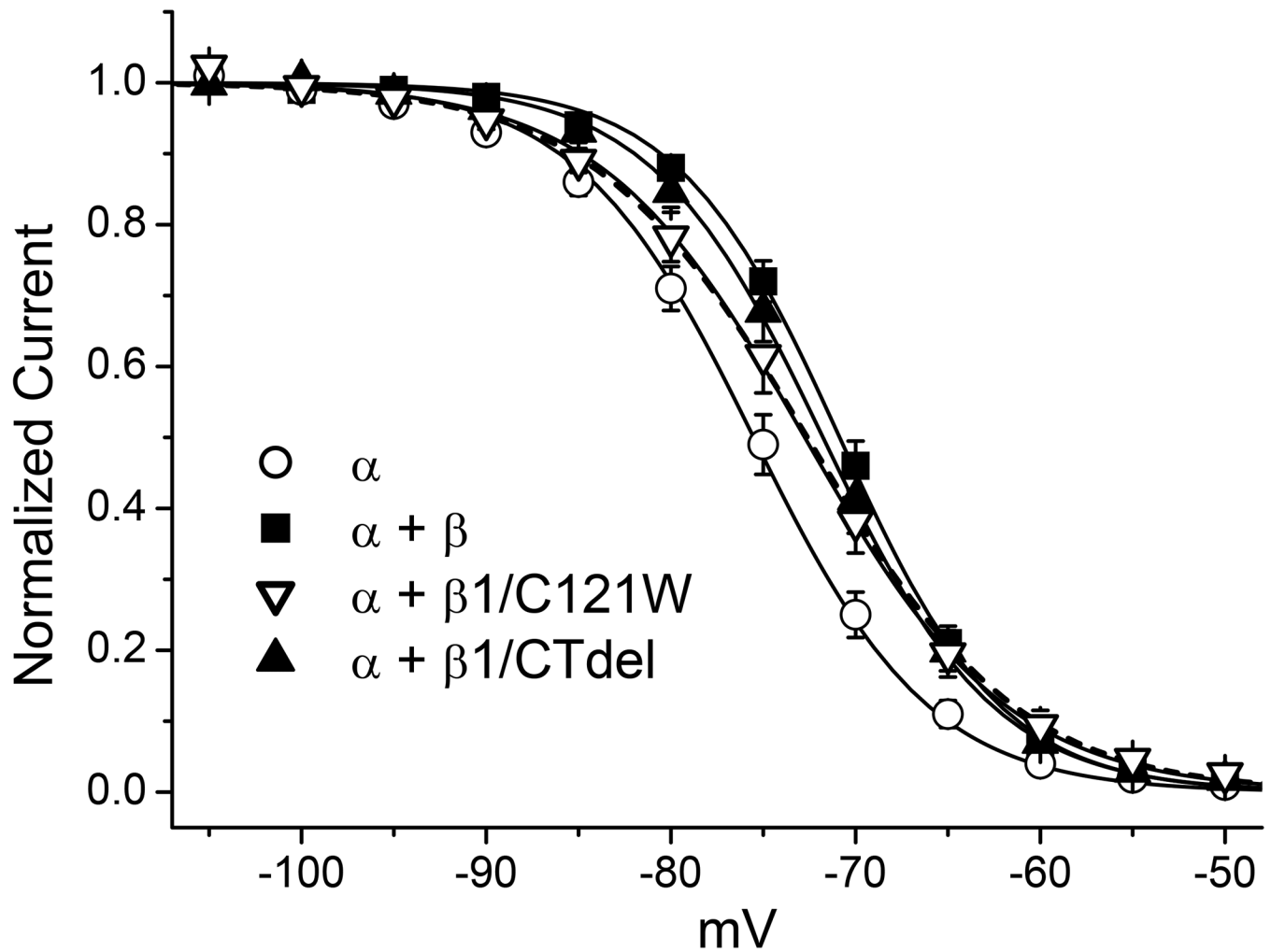
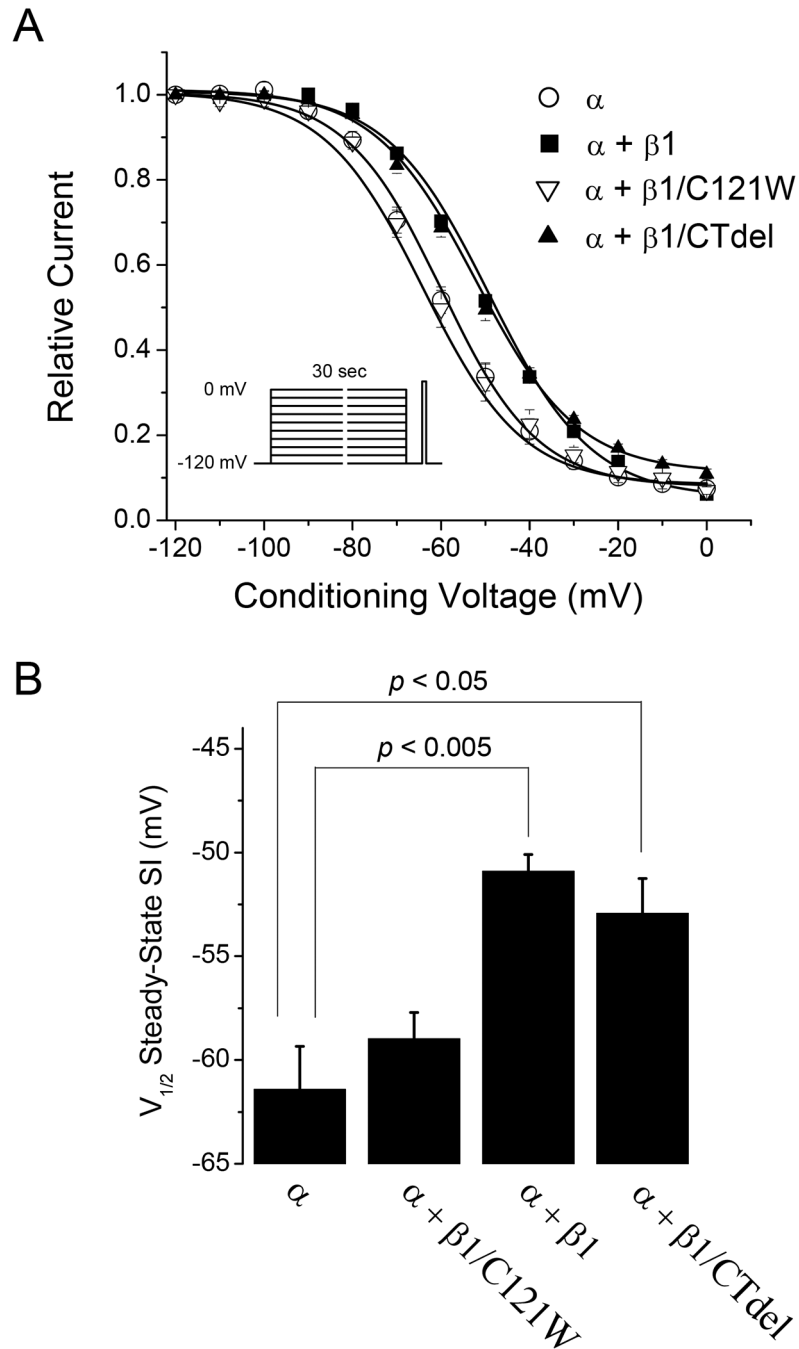


FIGURE 1.

Sodium channel activation was not altered by co-expression of wild-type or mutant sodium channel $\beta 1$ subunits. Sodium currents were elicited by a series of voltage steps from a holding potential of -120 mV to voltages ranging from -75 to $+75$ mV. (A) Representative current traces from cells expressing Nav1.4 α -subunit alone (α , ○); α plus wild-type $\beta 1$ ($\alpha + \beta 1$, ■); α plus $\beta 1$ N-terminal mutant C121W ($\alpha + \beta 1$ /C121W, ▽); and α plus $\beta 1$ C-terminal deletion ($\alpha + \beta 1$ /CTdel, ▲). (B) Normalized peak I-V curves show that the voltage-dependence of activation was not affected by coexpression of wild-type or mutant $\beta 1$ subunits.

**FIGURE 2.**

Voltage-dependence of fast inactivation was mildly disrupted by coexpression of $\beta1$. Voltage-dependence of fast inactivation was determined from test depolarizations to -10 mV immediately after a 300-ms conditioning pulse at potentials ranging from -120 to -50 mV. Coexpression of wild-type $\beta1$ ($\alpha + \beta1$, ■) caused a 5 mV rightward shift in $V_{1/2}$ of fast inactivation compared to α subunit alone (α , ○) ($p < 0.001$), and modestly decreased the slope factor (Table 1). $\beta1$ C-terminal deletion mutant ($\alpha + \beta1/CTdel$, ▲) effects were similar to wild-type $\beta1$ ($\alpha + \beta1$, ■). The N-terminal mutant ($\alpha + \beta1/C121W$, ▽) had an intermediate effect with a 3 mV shift of $V_{1/2}$, and an increased the slope factor compared to the α subunit alone ($p < 0.01$). Solid lines depict Boltzmann fits to the data with the parameter values listed in Table 1. The dashed line shows the fit with a sum of two Boltzmann functions to the $\alpha + \beta1/C121W$ data, with the constraint that the voltage midpoints for the two components are fixed at their values determined from fits to α only and $\alpha + \beta1$ WT. The sum is comprised of 60% with $\alpha + \beta1$ features ($V_{1/2}$ of -70.9 mV) and 40% monomeric α only ($V_{1/2}$ of -75.5 mV).

**FIGURE 3.**

The $\beta 1$ subunit mildly impedes steady-state slow inactivation. The voltage dependence of slow inactivation was measured as the peak current elicited by a test depolarization to -10 mV after 30-s conditioning pulses ranging from -120 to 0 mV (*inset*). Conditioning and test pulses were separated by a 20-ms recovery gap at -120 mV to remove fast inactivation. (A) Coexpression of the wild-type $\beta 1$ subunit ($\alpha + \beta 1$, ■) or the $\beta 1$ C-terminal deletion ($\alpha + \beta 1/CTdel$, ▲) depolarized (right-shifted) the voltage-dependence of steady-state slow inactivation compared to expression of α -subunit alone (α , ○) or coexpressed with the $\beta 1$

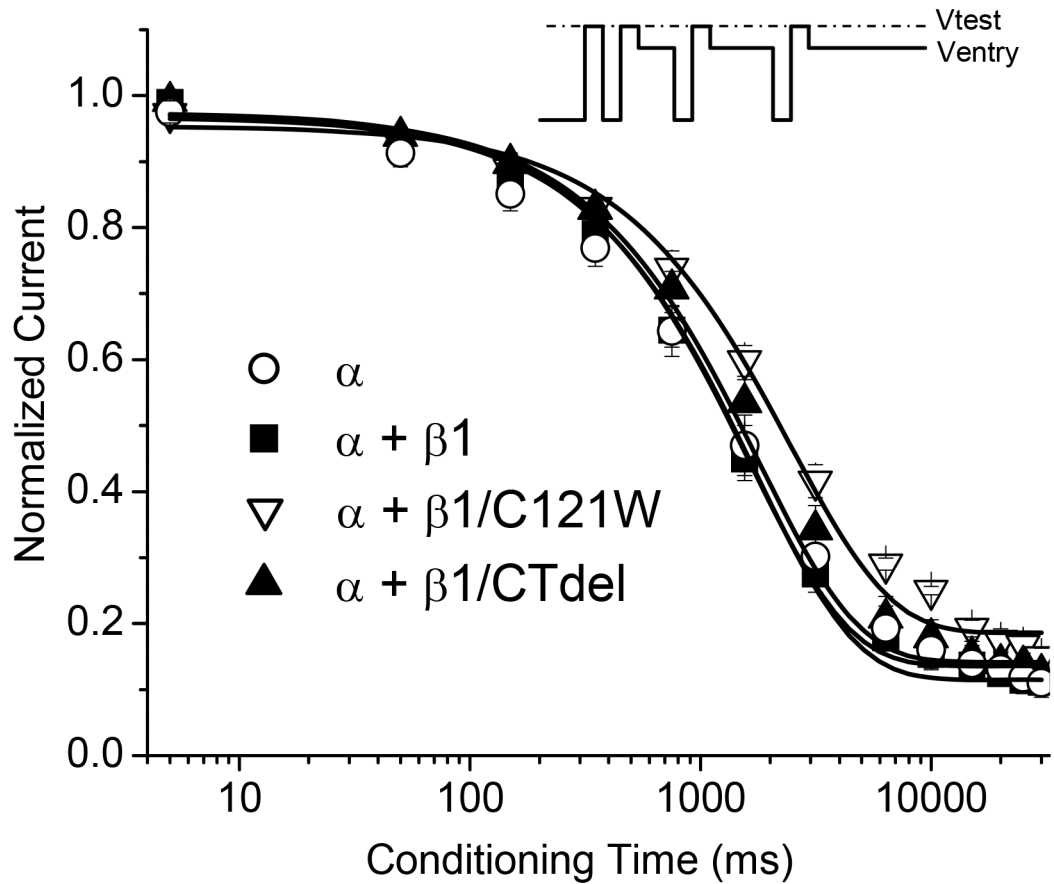
N-terminal mutation C121W ($\alpha + \beta 1/\text{C121W}$, ∇). (B) Voltage of half-inactivation ($V_{1/2}$) for steady-state slow inactivation was depolarized by $\sim 10\text{mV}$ upon coexpression of wild-type $\beta 1$ ($p < 0.005$), and $\beta 1/\text{CTdel}$ ($p < 0.05$) compared to α -subunit alone, while $V_{1/2}$ for $\beta 1/\text{C121W}$ was not significantly different.

Author Manuscript

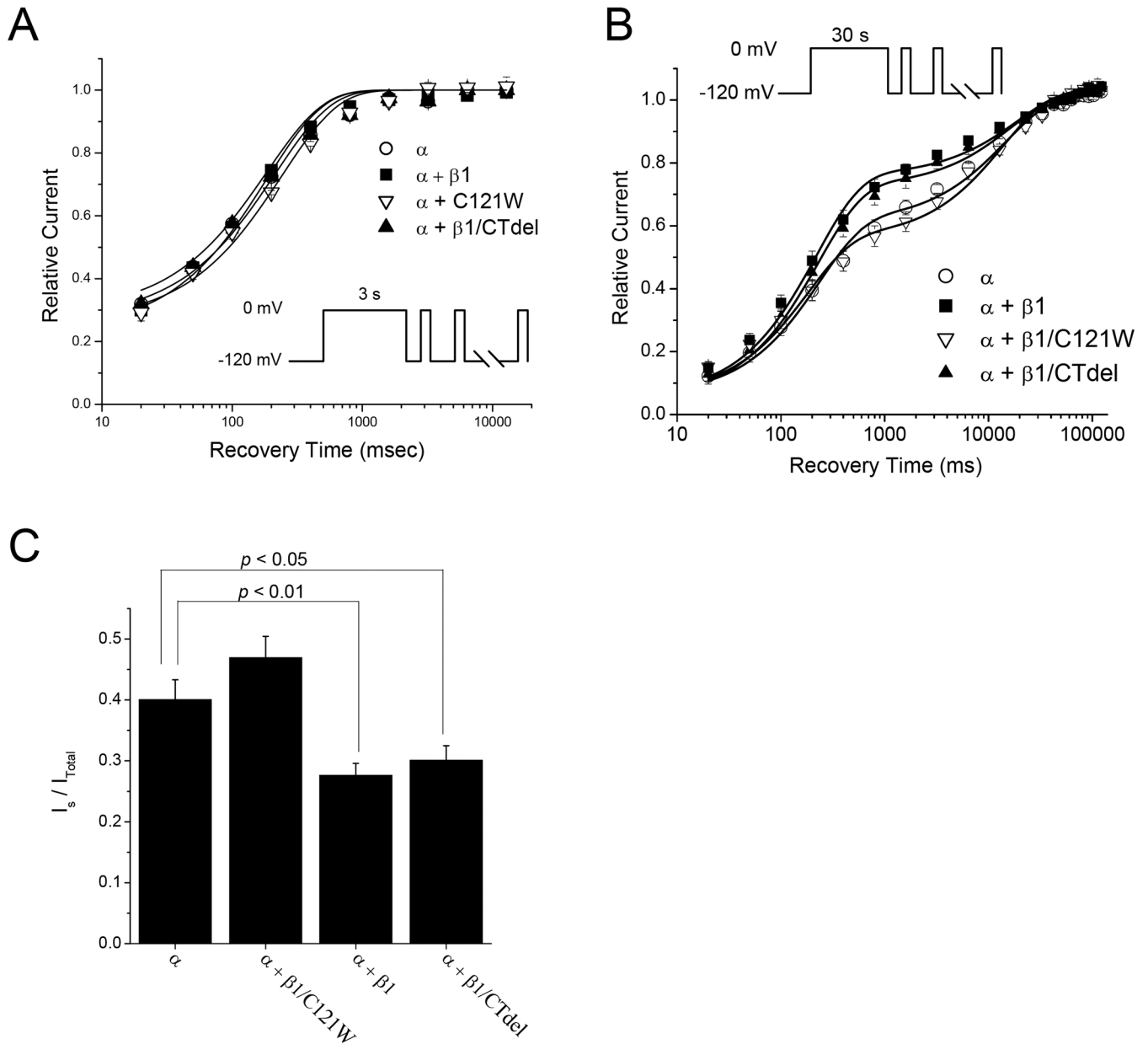
Author Manuscript

Author Manuscript

Author Manuscript

**FIGURE 4.**

The rate of entry to slow inactivation was not affected by coexpression of WT $\beta 1$, but was slightly prolonged by coexpression of $\beta 1/C121W$. Entry to slow inactivation at 0 mV was measured using a sequential entry protocol (*inset*). Expression of wild-type $\beta 1$ ($\alpha + \beta 1$, \blacksquare) or α and $\beta 1$ C-terminal deletion mutant ($\alpha + \beta 1/CTdel$, \blacktriangle) did not affect the rate of entry to slow inactivation, as compared to coexpression of α subunit alone (α , \circ). The $\beta 1$ N-terminal mutation C121W ($\alpha + \beta 1/C121W$, ∇) prolonged the rate of entry to slow inactivation by 1.4-fold ($p < 0.05$).

**FIGURE 5.**

The $\beta 1$ subunit preferentially disrupted the I_s component of slow inactivation. Recovery from slow inactivation at -120 mV was determined by applying a series of brief test depolarizations to -10 mV at progressively longer times after returning to -120 mV from either a 3 or 30-s conditioning pulse to 0 mV. (A) After a short (3-s) conditioning pulse recovery from slow inactivation was monoexponential with a time constant of ~ 200 ms, reflecting recovery from the intermediate inactivated (I_M) state. Coexpression of WT $\beta 1$ ($\alpha + \beta 1$, ■) or either $\beta 1$ subunit mutation ($\alpha + \beta 1/CTdel$, ▲; $\alpha + \beta 1/C121W$, ▽) did not affect the magnitude or the kinetics of recovery from the I_M state, relative to expression of α subunit alone (α , ○). Smooth curves show bi-exponential fits with the fast time constant set at a fixed value equal to that determined from the fast inactivation recovery protocol (Table

1). (B) Recovery after a longer (30-s) conditioning pulse showed two distinct kinetic components that reflected recovery from both the I_M and I_S states. Coexpression of wild-type $\beta 1$ did not alter recovery kinetics of either state, but decreased the relative proportion of channels partitioned into the I_S state compared to α -subunit alone ($p < 0.01$) (Table 2). The $\beta 1$ C-terminal deletion mutant yielded I_S results similar to WT $\beta 1$, while the $\beta 1/C121W$ mutant disrupted the $\beta 1$ effect on I_S , yielding results similar to expression of α -subunit alone. (C) Quantification of the percentage of channels recovering from the slow (I_S) component after 30-s conditioning pulses. Coexpression of α plus WT $\beta 1$ or $\beta 1/CTdel$ caused an ~25% reduction in channels occupying the I_S state relative to expression of α -subunit alone or $\alpha + \beta 1/C121W$ ($p < 0.05$).

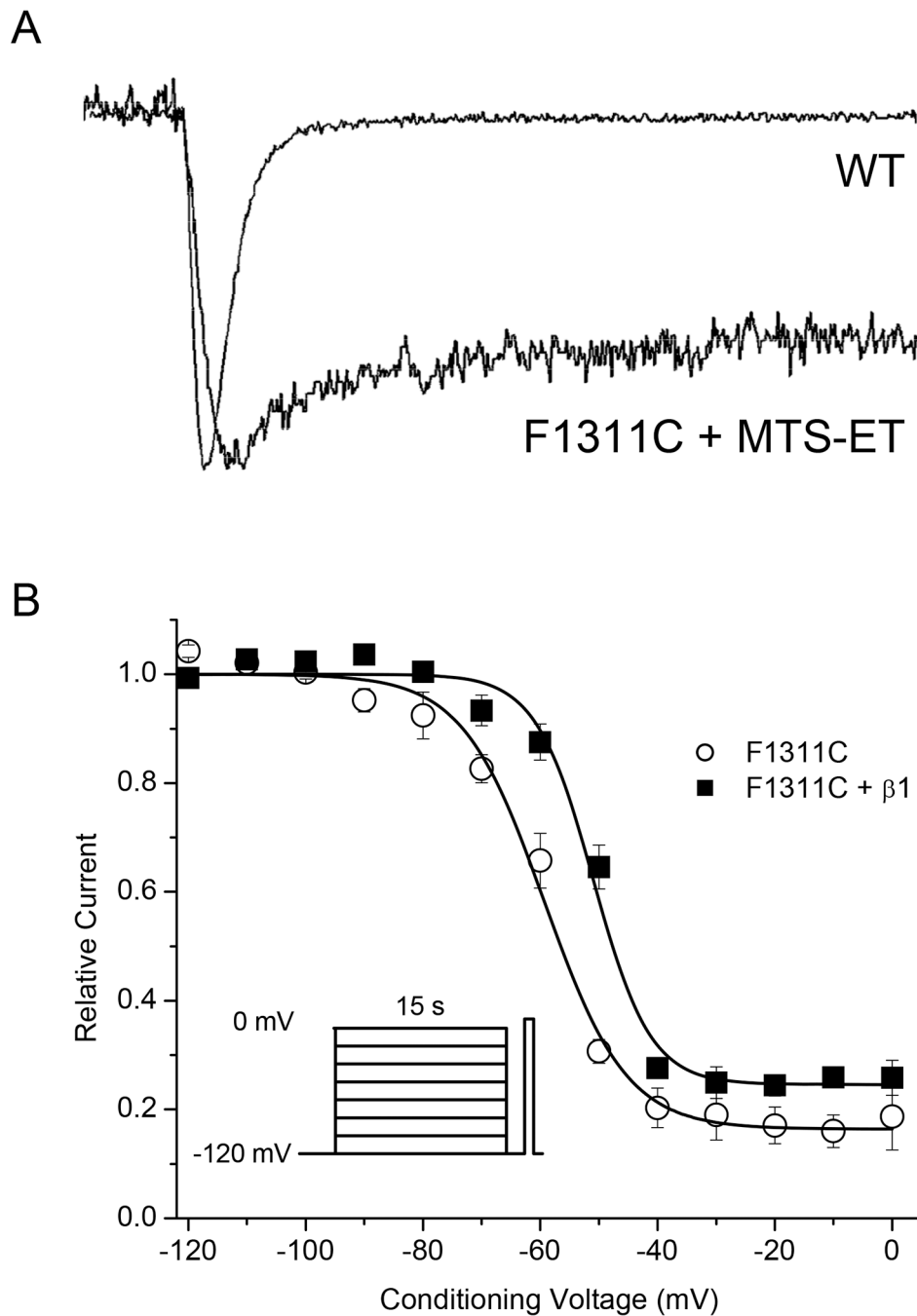


FIGURE 6. Disruption of fast inactivation did not abolish $\beta 1$ modulation of slow inactivation. Fast inactivation was severely disrupted by the α -subunit F1311C mutant when channels were exposed to 500 μ M internal MTS-ET. (A) Raw traces demonstrate the profound disruption of fast inactivation in the F1311C mutant exposed to internal MTS-ET. (B) In the absence of fast inactivation, coexpression of $\beta 1$ (F1311C + $\beta 1$, ■) caused an +11 mV depolarization (right-shift) in half-inactivation ($V_{1/2}$) of slow inactivation compared to expression of mutant

α -subunit alone/F1311C, O), $p < 0.005$. Steady-state slow inactivation was measured as described in Fig 3, except that a 15 s conditioning pulse was used.

Author Manuscript

Author Manuscript

Author Manuscript

Author Manuscript

Table 1.

Current Density and Fast Inactivation Gating Parameters

Channel Subunit	Peak Current at -15 mV pA/pF	$V_{1/2}$ mV	k mV	τ_{recovery} msec
α	-96.9 ± 17 (15)	-75.5 ± 0.80 (10)	4.8 ± 0.18 (10)	2.0 ± 0.10 (10)
$\alpha + \beta 1$	-136 ± 23 (7)	-70.9 ± 0.62 (6)**	4.4 ± 0.08 (6)	1.9 ± 0.07 (6)
$\alpha + \beta 1/\text{C121W}$	-85.0 ± 21 (7)	-72.5 ± 1.1 (6)	5.5 ± 0.26 (6)*	2.0 ± 0.15 (5)
$\alpha + \beta 1/\text{CTdel}$	-80.6 ± 14 (9)	-71.8 ± 0.91 (6)*	4.6 ± 0.14 (6)	2.0 ± 0.08 (4)

Values are means \pm SEM with the number of observations in parentheses.

* Statistically different from α -subunit only at $p < 0.01$.

** Statistically different from α -subunit only at $p < 0.001$

Table 2.

Kinetics of Recovery from Slow Inactivation

Channel Subunit	3 – second conditioning pulse			30 – second conditioning pulse		
	τ_M msec	I_M	τ_M msec	I_M	τ_S sec	I_S
α	210 ± 15	0.73 ± 0.02	230 ± 50	0.55 ± 0.03	15 ± 1.6	0.40 ± 0.03
$\alpha + \beta 1$	180 ± 5.5	0.77 ± 0.02	220 ± 32	0.70 ± 0.03*	19 ± 4.0	0.28 ± 0.02**
$\alpha + \beta 1/C12IW$	240 ± 11	0.74 ± 0.04	180 ± 20	0.50 ± 0.02	14 ± 1.6	0.47 ± 0.03
$\alpha + \beta 1/CTdel$	180 ± 11	0.71 ± 0.03	230 ± 25	0.67 ± 0.03*	17 ± 2.9	0.30 ± 0.02*

Values are means ± SEM; N = 5 for all channel types except for $\alpha + \beta 1$ in which N = 6.

* Statistically different from α -subunit only at $p < 0.05$.

** Statistically different from α -subunit only at $p < 0.01$